

Innovative Hydrocyclone Inlet Designs To Reduce Erosion-Induced Wear In Mineral Dewatering Processes

Peng Xu and Arun S. Mujumdar



TABLE OF CONTENT

ABSTRACT..... 2

1. INTRODUCTION..... 2

2. MODEL DESCRIPTION..... 7

2.1 TURBULENCE MODEL..... 7

2.1.1 k-ε Model..... 7

2.1.2 Reynolds Stress Model..... 9

2.1.3 Large Eddy Simulation..... 11

2.2 MULTIPHASE MODEL..... 13

2.3 PARTICLE TRACKING..... 15

2.4 EROSION MODEL..... 16

3. SIMILATION..... 17

4. MODEL VALIDATION..... 19

4.1 FLUID FLOW FIELD..... 19

4.2 FORMATION OF THE AIR CORE..... 21

5. EROSION RATE..... 25

6. CONCLUDING REMARKS..... 28

ACKNOWLEDGEMENTS..... 29

REFERENCES..... 29

M3TC Technical Report TN-08-01

Innovative Hydrocyclone Inlet Designs to Reduce Erosion-induced Wear in Mineral Dewatering Processes

Peng Xu and A.S. Mujumdar

Abstract

The hydrocyclone is a mechanical separation device which is used widely in mineral processing. The solid particles in mineral slurries are separated according to their density, size and shape by the centrifugal force generated by an induced vortex motion in a cylinder-on-cone vessel. The larger and denser particles move closer to the wall region due to their greater inertia and descend by gravity; a higher concentration suspension is thus collected at the bottom of the hydrocyclone. While the cleaned liquid and hydrodynamically smaller particles exit through an overflow outlet at the top of the hydrocyclone. Higher velocities, within limit, generally yield higher collection efficiency. However, higher stream velocities cause severe erosion of the internal wall of hydrocyclones as mineral slurries generally are abrasive. The objective of this study is to use the computational fluid dynamic (CFD) technique to model the turbulent swirling flow and predict regions of significant wear and how they are influenced by design of the inlet ducting. New inlet designs are proposed and investigated numerically for their erosion characteristics, pumping power requirements and collection efficiency. Successful innovation in hydrocyclone design will lead to reduced maintenance and lower operating energy costs in mineral processing.

Keywords: Hydrocyclone; Computational fluid dynamics; Turbulence model; Air core; Erosion rate

1. Introduction

The hydrocyclone is an important and popular industrial apparatus to separate by centrifugal action dispersed solid particles from a liquid suspension fed to it. It is widely used in industry, particularly in the mineral and chemical processing industries because of its simplicity in design and operation, high capacity, low maintenance and operating costs as well as its small physical size (Bradley, 1965; Svarovsky, 1984). Recently, the application of hydrocyclone in the wet process

M3TC Technical Report TN-08-01

of beneficiation has attracted more interest with the current boom in advanced mineral processing driven by the expanding mineral commodities markets and escalating energy costs. In this work, we focus on the application of the hydrocyclone in mineral processing with a CFD model specially constructed to predict erosion rates. We expect such a model to assist as a design and analysis tool to arrive at better designs which suffer lower erosion rates. Although clearly very important from an economic standpoint this area which has received little attention in the literature on hydrocyclones.

A typical hydrocyclone consists of a cylindrical section with a central tube connected to a conical section with a discharge tube. An inlet tube is attached to the top section of the cylinder. The cone angle of the conical section varies widely in practice from 5° to 40° . There are two axial product outlets. The spigot is situated at the apex of the conical part and the vortex finder is located at the upper end of the cylindrical section and contains a tubes extending into the hydrocyclone. The tangentially injected fluid causes swirl, and the centrifugal force field so generated brings about separation of the particulate material from the medium in which it is suspended, based mainly on particle density, size and shape. Particles of sufficiently high settling velocity are centrifuged to the walls of the hydrocyclone and drained off as a concentrated solution through the spigot. Particles with a low settling velocity are carried away by an upward vortex which forms around the cyclone axis and is drained off by the vortex finder.

Although many efforts have been made to study experimentally the flow in hydrocyclones (Yoshioka and Hotta, 1955; Lilge, 1962; Bradley, 1965; Svarovsky, 1984), little detailed flow information was generated until the availability of Laser Doppler Anemometry (LDA) necessary to measure local fluid velocities within the hydrocyclone (Dabir and Petty, 1986; Hsieh and Rajamani, 1991; Dai et al., 1999). It is well known that the LDA technique is expensive, largely limited to the dispersed liquid phase, and at present suitable only for laboratory scale studies rather than industrial design and application. Hence empirical equations/models are often used by designers

of hydrocyclones. However, empirical equations/models suffer from their inherent deficiency as they can only be used within the limits of the experimental data from which the empirical parameters were determined. No innovative changes can be predicted with empirical modeling. In view of these shortcomings, mathematical models based on the basic fluid mechanics are highly desirable to intensify innovation.

The CFD technique is gaining popularity in process design and optimization as it provides a good means of predicting equipment performance of the hydrocyclone under a wide range of geometric and operating conditions; it also offers an effective way to design and optimize the hydrocyclones. The first CFD model utilizing the standard k - ϵ turbulence model for a hydrocyclone was developed by Boysan et al. (1982). The k - ϵ turbulence model intrinsically makes the assumption that the turbulence is isotropic because only one scalar velocity fluctuation is modeled. Furthermore, the Boussinesq approximation on which the eddy viscosity intrinsically relies implies equilibrium between stress and strain. Therefore, the k - ϵ turbulent model is not suitable to simulate a turbulent flow with high swirl, flow reversal and/or flow separation (Ma et al., 2000). Many authors have adopted the renormalization group (RNG) k - ϵ model with a swirl correction to enhance the precision of simulations because it includes additional terms for the dissipation rate, ϵ , development which significantly improves the accuracy for rapidly strained flows (Fraser et al., 1997; He et al., 1999; Schuetz et al., 2004; Narasimha et al., 2005). However, Suasnabar (2000) found that the swirl constant in the RNG k - ϵ model needs to be increased to improve predictions; this in turn can cause numerical instability. Therefore, the application of the RNG k - ϵ model is also limited for modeling a hydrocyclone. The Reynolds stress model (RSM) solves the transport equation for each individual Reynolds stress, which enables RSM to model anisotropic turbulence and strained flows where the Boussinesq approximation is known to be invalid. Some recent studies indicate that RSM can improve accuracy of the numerical solution (Cullivan et al., 2003; Cullivan et al., 2004; Brennan, 2006; Narasimha et al., 2006; Wang et al., 2007). However, the

predictions are not what they could be and there is debate about appropriate modeling options. Recent advances in computational power have begun to make large eddy simulation (LES) practical for engineering problems. LES is intrinsically a dynamic simulation and can capture time-dependent vortex oscillations and nonequilibrium turbulence, which suggest that it should be appropriate for modeling hydrocyclone. Comparing with other turbulence models, LES provides better predictions including velocity, air core and separation efficiency (Souza and Neto, 2004; Brennan, 2006; Narasimha et al., 2006; Delgadillo and Rajamani, 2005; Delgadillo and Rajamani, 2007). Certainly, LES simulations of large industrial dense medium hydrocyclone will be computationally impractical except for a test case (Narasimha et al., 2006).

A striking feature of the flow field is the presence of an air core in the hydrocyclone. At the central axis of the hydrocyclone, the low pressure developed supports formation of a rotating air column called the air core. The geometry and the stability of the air core have been empirically found to have a strong influence on the performance of the hydrocyclone (Svarovsky, 1984; Narasimha et al., 2006). In the mineral processing field, the air core dimension is a critical variable, since a large air core diameter leads to a condition known as "roping". As the interface between liquid and air phases is difficult to determine, the nature of air core is often neglected in many previous CFD modeling efforts (Nowakowski et al., 2004; Souza and Neto, 2004). or they work with a simplified assumption about its formation and behavior (Monredon et al., 1992; Rajamani and Devulapalli, 1994). The volume-of-fluid (VOF) model has been proven to be an effective method for modeling the air core and predicting the formation and shape of air core (Cullivan et al., 2003; Cullivan et al., 2004; Delgadillo and Rajamani, 2005; Brennan, 2006; Narasimha et al., 2006; Delgadillo and Rajamani, 2007; Wang et al., 2007). For solids movement, an Eulerian-Lagrangian model has been successfully applied to dilute flow phenomena in a hydrocyclone (Ma et al., 2000). In the last several decades, this field had advanced so much that Slack et al. (2003) proposed an automated tool for novice analysts to carry out simulations with standard CFD packages.

There is analogy between CFD modeling of liquid-particle swirling flow in a hydrocyclone and gas-droplet/particle flow that occurs in a cylinder-on-cone spray dryer. The latter includes heat and mass transfer which is not present in classification in a hydrocyclone which is a purely fluid dynamic problem. Interested readers are referred to the work of Huang et al. (2003, 2004, 2006) provides some useful insight into the relative performance of various turbulence models applied to swirling two-phase flow

Erosion of parts of the internal wall of the hydrocyclone is a critical issue in mineral dewatering both from both safety and economic considerations. The injected solids particles, such as sand and ore particles, impinge the inside surfaces of the components of the hydrocyclone, causing mechanical wear and eventual failure of the devices. Therefore, the ultimate goal in the design of hydrocyclone is not only to provide better performance, but also to be resistant to wear. As testing for erosion of industrial devices generally requires special equipment and methodology, CFD modeling has been widely adopted as an effective tool to predict the wear response at low price and without costly experimentation (Bozzini et al., 2003; Mazur et al., 2004; Chen et al., 2004; Amezcua et al., 2007; Sciubba and Zeoli, 2007). Although CFD modeling has been tested to estimate the erosion rate in a hydrocyclone with one novel inlet design, the results found in literature are very few and largely preliminary; they do not indicate in detail the effect of flow and geometry on the erosion rate (Olson and Ommen, 2004). Hence further modeling effort is needed for advancing our capability in predicting wear of hydrocyclones.

This work presents a CFD model of a hydrocyclone based on Fluent version 6.3. First, results using different turbulence models viz. $k-\epsilon$, RSM and LES, are compared with published experimental results for a 75mm standard hydrocyclone (Hsieh, 1988). The air core geometry is predicted using a VOF multiphase model. Then, the erosion rate for four designs of a 75mm hydrocyclone fitted with different inlets is calculated. This paper is organized into six sections. Section 2 describes the CFD model including the turbulence models, the multiphase model, the

particle tracking model and the erosion model. Section 3 explains the numerical methodology and initial and boundary conditions. Section 4 shows a comparison of simulated results with experimental data. Section 5 illustrates the predicted erosion rates and discusses the influence of inlet geometry on the erosion rate in the modeled hydrocyclone. The last section includes discussion with conclusions and future prospects.

2. Model Description

2.1 Turbulence Model

The turbulence model is the key component in the description of the fluid dynamics of the hydrocyclone. The free surface, air core and solid particles make the rotating turbulent flow more anisotropic, which adds difficulty for modeling hydrocyclone with CFD. Three kinds of turbulence model-k- ϵ , RSM and LES are often adopted for modeling the turbulence in hydrocyclone. The 75mm standard hydrocyclone is simulated with different turbulence models and the numerical results are also compared with Hsieh's experimental results [36] to validate the CFD model.

2.1.1 k- ϵ model

In mineral processing, the fluid suspensions are generally dilute (<10%), thus the incompressible Navier-Stokes equations supplemented by a suitable turbulence model are appropriate for modeling the flow in hydrocyclone. And the velocity components are decomposed into the mean \bar{v} and fluctuating v' velocities.

$$v_i = \bar{v}_i + v'_i \quad (1)$$

$$\frac{\partial \rho}{\partial t} + \rho \frac{\partial \bar{v}_i}{\partial x_i} = 0 \quad (2)$$

$$\frac{\partial(\rho\bar{v}_i)}{\partial t} + \frac{\partial(\rho\bar{v}_i\bar{v}_j)}{\partial x_j} = -\frac{\partial p}{\partial x_i} + \frac{\partial}{\partial x_j} \left(\mu \frac{\partial \bar{v}_i}{\partial x_j} \right) + \frac{\partial}{\partial x_j} (-\rho\bar{v}'_i\bar{v}'_j) + \rho g_i \quad (3)$$

where $-\rho\bar{v}'_i\bar{v}'_j$ ($i=1,2,3$) is the Reynolds stress term and includes the turbulence closure, which must be modeled in order to close Eq. (3). Eqs. (2) and (3) are steady-state conservation equations of mass and momentum, respectively. For the Reynolds stress term, there are different models which can be used to describe this term. For example, k- ϵ and RSM models have been applied in hydrocyclone with a great degree of success.

The k- ϵ model is a semi-empirical model based on model transport equations for turbulence kinetic energy k and its dissipation rate ϵ with the assumption that the flow is fully turbulent and the effects of molecular viscosity are negligible. It calculates the Reynolds stresses using an eddy viscosity which is in turn calculated from the solved k and ϵ . Comparing with standard k- ϵ model, the renormalization group (RNG) k- ϵ model includes additional terms for dissipation rate ϵ development which can significantly improve the accuracy for rapidly strained flows (Yakhot and Ozag, 1986). The effect of swirl on turbulence is included in the RNG k- ϵ model, enhancing accuracy for swirling flows. The turbulence kinetic energy k and its dissipation rate ϵ in RNG k- ϵ model can be obtained from the following equations:

$$\frac{\partial(\rho k)}{\partial t} + \frac{\partial(\rho k v_i)}{\partial x_i} = \frac{\partial}{\partial x_j} (\alpha_k \mu_{eff} \frac{\partial k}{\partial x_j}) + G_k + G_b - \rho \epsilon - Y_M + S_k \quad (4)$$

$$\frac{\partial(\rho \epsilon)}{\partial t} + \frac{\partial(\rho \epsilon v_i)}{\partial x_i} = \frac{\partial}{\partial x_j} (\alpha_\epsilon \mu_{eff} \frac{\partial \epsilon}{\partial x_j}) + C_{1\epsilon} \frac{\epsilon}{k} (G_k + C_{3\epsilon} G_b) - C_{2\epsilon} \rho \frac{\epsilon^2}{k} - R_\epsilon + S_\epsilon \quad (5)$$

In Eqs. (4) and (5), G_k and G_b are the generations of turbulence kinetic energy due to the mean velocity gradients and buoyancy respectively, and Y_M represents the contribution of the fluctuating dilatation in compressible turbulence to the overall dissipation rate. The quantities α_k

and α_ε are the inverse effective Prandtl numbers for k and ε , respectively. S_k and S_ε are user-defined source terms, and $C_{1\varepsilon}$, $C_{2\varepsilon}$ and $C_{3\varepsilon}$ are constants.

The RNG k- ε model provides an option to account for the effects of swirl or rotation by modifying the turbulent viscosity appropriately. The modification takes the following functional form:

$$\mu_t = \mu_{t0} f(\alpha_s, \Omega, \frac{k}{\varepsilon}) \quad (6)$$

where μ_{t0} is the value of turbulent viscosity calculated without the swirl modification, Ω is a characteristic swirl number, and α_s is a swirl constant that assumes different values depending on whether the flow is swirl-dominated or only mildly swirling. The swirl modification always takes effect for axisymmetric, swirling flow and three-dimensional flow. The default value of swirl constant in Fluent is set for mildly swirling flow, thus, the it has to be increased for strongly swirling flow in order to improve predictions, which will cause numerical instability (Suasnabar, 2000). The additional term R_ε in the ε equation (Eq. (5)) is the main difference between the standard and RNG k- ε models. The RNG k- ε model is more responsive to the effects of rapid strain and streamline curvature than the standard k- ε model, which explains the superior performance of the RNG k- ε model for high swirling flow in hydrocyclone. Furthermore, the adoption of μ_{eff} allows the RNG k- ε model to better handle low Reynolds number and near wall flows.

2.1.2 Reynolds Stress Model

The Reynolds stress model (RSM) closes the Reynolds-averaged Navier-Stokes equations (RANS, see Eqs. (2) and (3)) by solving transport equations for the individual Reynolds stresses without isotropic eddy-viscosity hypothesis and together with an equation for the dissipation rate. Since the RSM accounts for the effects of streamline curvature, swirl, rotation, and rapid changes in

strain rate in a more rigorous manner, it has greater potential to give accurate predictions for complex flows in hydrocyclone. The RSM has been proven to be an appropriate turbulence model for hydrocyclone (Cullivan et al., 2003; Cullivan et al., 2004; Narasimha et al., 2006; Wang et al., 2007).

The exact transport equations for the transport of the Reynolds stress term $\overline{\rho v'_i v'_j}$ (see Eq. (3)) in RSM are written as:

$$\frac{\partial(\overline{\rho v'_i v'_j})}{\partial t} + \frac{\partial(\overline{\rho v'_k v'_i v'_j})}{\partial x_k} = D_{T,ij} + P_{ij} + \phi_{ij} + \varepsilon_{ij} \quad (7)$$

The four terms in the right of Eq. (7) are the turbulent diffusion $D_{T,ij}$, stress production P_{ij} , pressure strain ϕ_{ij} and dissipation ε_{ij} , which can be expressed by Eqs. (8)-(11).

$$D_{T,ij} = -\frac{\partial}{\partial x_k} [\overline{\rho v'_i v'_j v'_k} + \overline{p(\delta_{kj} v'_i + \delta_{ik} v'_j)}] \quad (8)$$

$$P_{ij} = -\overline{\rho(v'_i v'_k \frac{\partial v'_j}{\partial x_k} + v'_j v'_k \frac{\partial v'_i}{\partial x_k})} \quad (9)$$

$$\phi_{ij} = \overline{p(\frac{\partial v'_i}{\partial x_j} + \frac{\partial v'_j}{\partial x_i})} \quad (10)$$

$$\varepsilon_{ij} = -2\overline{\mu \frac{\partial v'_i}{\partial x_k} \frac{\partial v'_j}{\partial x_k}} \quad (11)$$

where δ is the Kronecker factor. In the simulation process of hydrocyclone, the standard linear pressure strain (LPS) model (Launder et al., 1975) and quadratic pressure strain (QPS) model (Speziale et al., 1991) are often adopted. Narasimha et al. (2006) stated that the constants in the LPS correlation need to be adjusted to match the velocity predictions with data. Comparing with the default LPS model, the QPS model has been demonstrated to give superior performance in a

range of basic shear flow, including plane strain, rotating plane shear, and axisymmetric expansion/contraction. This improved accuracy should be beneficial for the complex flows in hydrocyclone (Cullivan et al., 2003). Therefore, the QPS RSM is chosen in the current simulation.

2.1.3 Large Eddy Simulation

Large eddy simulation (LES) provides an alternative approach in which large eddies are explicitly resolved in a time-dependent simulation using the filtered Navier-Stokes equations. Velocity profiles of LES are resolved by a filtering operation of the velocity field, and the smaller scales or residuals are modeled in a particular manner. The velocity field is defined as the sum of the filtered velocity \bar{v}_i and the residual component \bar{v}'_i ,

$$v_i = \bar{v}_i + \bar{v}'_i \quad (12)$$

Applied Eq. (12) to the governing Navier-Stokes equations, the filtered Navier-Stokes equations are obtained, where an additional stress tensor appears.

$$\frac{\partial \rho}{\partial t} + \rho \frac{\partial \bar{v}_i}{\partial x_i} = 0 \quad (13)$$

$$\frac{\partial(\rho \bar{v}_i)}{\partial t} + \frac{\partial(\rho \bar{v}_i \bar{v}_j)}{\partial x_j} = -\frac{\partial p}{\partial x_i} + \frac{\partial}{\partial x_j} \left(\mu \frac{\partial \bar{v}_i}{\partial x_j} \right) - \frac{\partial \tau_{ij}^{sgs}}{\partial x_j} + \rho g_i \quad (14)$$

The filtered Navier-Stokes equations account for the transfer of momentum by subgrid scales of turbulence. The subgrid-scale stress τ_{ij}^{sgs} is defined as

$$\tau_{ij}^{sgs} \equiv \overline{\rho v_i v_j} - \rho \bar{v}_i \bar{v}_j \quad (15)$$

The subgrid-scale stresses resulting from the filtering operation are unknown, and require modeling. The subgrid-scale stresses are usually modeled using a simple eddy viscosity, that is the stresses are defined as the product of the eddy viscosity and the strain rate,

$$\tau_{ij}^{sgs} \equiv \rho \mu_t \left(\frac{\partial \bar{v}_i}{\partial x_j} + \frac{\partial \bar{v}_j}{\partial x_i} \right) \quad (16)$$

The simplest subgrid-scale model is the Smagorinsky-Lilly model (SLM) (Smagorinsky, 1963). This model proposes that the subgrid-scale eddy viscosity is related to the local average grid spacing and the mean strain rate. The Fluent implementation makes the length scale equal to the distance from the wall d in wall bounded regions:

$$\mu_t = \rho L_s^2 \sqrt{2 \bar{S}_{ij} \bar{S}_{ij}} \quad (17)$$

where \bar{S}_{ij} is the strain rate and the mixing length for subgrid scales can be calculated by

$$L_s = \min(\kappa d, C_s V^{1/3}) \quad (18)$$

where κ is the von Kármán constant, C_s is the Smagorinsky constant, and V is the volume of the computational cell. The Smagorinsky constant is not an universal constant, which is the most serious shortcoming of this simple model. Narasimha et al. (2006) and Brennan (2006) adopted the SLM subgrid-scale model and took the Smagorinsky constant as the default value 0.1 in their large eddy simulation of hydrocyclone, and their numerical results give good agreement with experimental results.

LES is not well defined to solve the flow close to the walls. The renormalization group (RNG) subgrid-scale model (Yakhot et al., 1989) is very effective to model the low-Reynolds-number effects encountered in transitional flows and near-wall regions where the molecular viscosity has more significance. The turbulent viscosity is defined as the difference between the effective viscosity and the molecular viscosity:

$$\mu_t = \mu_{eff} - \mu \quad (19)$$

While the effective viscosity is defined as,

$$\mu_{eff} = \mu[1 + H(x)]^{1/3} \quad (20)$$

where $H(x)$ is the Heaviside function defined as $H(x) = x$ for $x \geq 0$ and 0 for $x \leq 0$, and x can be expressed as $x = \mu_s^2 \mu_{eff} / \mu^3 - 100$. The turbulent viscosity, μ_s , in the subgrid scale is defined as:

$$\mu_s = (C_{RNG} V^{1/3})^2 \sqrt{2 \bar{S}_{ij} \bar{S}_{ij}} \quad (21)$$

Delgadillo et al. (2005, 2006, 2007) have used the RNG subgrid-scale model in the large eddy simulation of hydrocyclone, and they stated that the RNG LES model captures the dynamics of the flow in hydrocyclone and they have also proven that $C_{RNG} = 0.157$ is the most acceptable value (Delgadillo, 2006). It should be pointed out that LES model requires highly accurate spatial and temporal discretization, finer mesh than a comparable RANS simulation, and more compute resources. And also, there are still unanswered questions about appropriate subgrid-scale models for the multiphase flows encountered in mineral processing applications.

Therefore, four CFD models, RNG k- ϵ , QPS RSM, and SLM and RNG LES will be performed in 75mm standard hydrocyclone. And the numerical results will be compared with each other and that of experiment.

2.2 Multiphase Model

In the hydrocyclone, the centrifugal force generated by the tangential acceleration pushes the fluid to the wall and creates a low pressure in the central axis, which gives the right conditions to suck air into the device and form an air core. In the current simulation, the formation process, location and shape of the air core will be taken into account instead of neglecting it or making simple assumptions. The volume of fluid (VOF) free surface model is a simplification of the mixture model and has been successfully applied in predicting and modeling the air core in hydrocyclone

(Cullivan et al., 2003; Cullivan et al., 2004; Delgadillo and Rajamani, 2005; Brennan, 2006; Narasimha et al., 2006; Delgadillo and Rajamani, 2007; Wang et al., 2007). The VOF model can simulate two or more immiscible fluid phases, in which the position of the interface between the fluids is of interest. In VOF method, the variable density equations of motion are solved for the mixture, and an additional transport equation for the volume fraction of each phase is solved, which can track the interface between the air core and the liquid in hydrocyclone. The single momentum equation is solved throughout the domain, and the resulting velocity field is shared among the phases. This momentum equation, shown below, is dependent on the volume fractions of all phases through the properties ρ and μ .

$$\frac{\partial(\rho v_i)}{\partial t} + \frac{\partial(\rho v_i v_j)}{\partial x_j} = -\frac{\partial p}{\partial x_i} + \frac{\partial}{\partial x_j} [\mu (\frac{\partial v_i}{\partial x_j} + \frac{\partial v_j}{\partial x_i})] + \rho g_i \quad (22)$$

where ρ is the average density and can be calculated according to the density of q^{th} phase ρ_q and its volume fraction α_q which varies between 0 and 1, as,

$$\rho = \sum \alpha_q \rho_q \quad (23)$$

The transport equation for the volume fraction of each phase is

$$\frac{\partial \alpha_q}{\partial t} + v_j \frac{\partial \alpha_q}{\partial x_j} = 0 \quad (24)$$

The simple VOF model has been adopted by most engineers for modeling the air core in hydrocyclone. And the comparison of Eulerian multiphase model and VOF by Brennan (2006) indicates that the velocity predictions using the two models are essentially the same. Therefore, the air core will be resolved with VOF model in the current simulation. But for the dense slurry, the more sophisticated Eulerian multiphase model will be more suitable.

2.3 Particle Tracking

In most mineral processing operations, the solid phase is sufficiently dilute (<10%). Hence we can employ the discrete phase model (DPM), the fundamental assumption of which is that the dispersed second phase occupies a low volume fraction can be used to track solid particle movement. The Lagrangian DPM follows the Euler-Lagrange approach. The fluid phase is treated as a continuum by solving the time-averaged Navier-Stokes equations, while the dispersed phase is solved by tracking a large number of particles through the calculated flow field. The dispersed phase can exchange momentum, mass, and energy with the fluid phase.

The particle trajectories are computed individually at specified intervals during the fluid phase calculation. It can be predicted by integrating the buoyancy force and liquid drag force on the particle in a Lagrangian reference frame.

$$\frac{dv_p}{dt} = F_D(v - v_p) + \frac{g(\rho_p - \rho)}{\rho_p} \quad (25)$$

where v and v_p are velocity of fluid phase and particle, ρ and ρ_p are density of fluid and particle. $F_D(v - v_p)$ is the drag force per unit particle mass and

$$F_D = \frac{18\mu}{\rho_p d_p^2} \frac{C_D \text{Re}}{24} \quad (26)$$

where d_p is the particle diameter, the particle Reynolds number is defined as $\text{Re} \equiv \rho d_p |v_p - v| / \mu$, and C_D is the drag coefficient.

The dispersion of particles can be accounted for with a stochastic tracking model, in which the turbulent dispersion of particles is predicted by integrating the trajectory equations for individual particles and using the instantaneous fluid velocity. Also, unsteady tracking is used, where at the end of each time step the trajectory is updated with the instantaneous velocity. As for the slurry

feed concentrations in excess of 10% by volume, the DPM is not suitable and Eulerian multiphase model is more appropriate for tracking particles in hydrocyclone.

2.4 Erosion Model

The impingement of solid particles with hydrocyclone walls can cause considerable wear, which is an issue of great industrial concern, both from safety and economic considerations. The damage induced by the erosion can cause equipment failure. Hence, estimation of potential erosion of the hydrocyclone wall is important to predict the lifetime of the equipment; it is useful to know how it is affected by geometry and different operating conditions. Because of experimental difficulties, CFD analysis is an effective tool to investigate the erosion rate of hydrocyclone.

Particle erosion and accretion rates can be computed at wall boundaries based on the following model equations. The erosion rate is defined as (Fluent, 2006)

$$R_{erosion} = \sum_{p=1}^N \frac{\dot{m}_p C(d_p) f(\alpha) v^{b(v)}}{A} \quad (27)$$

where $C(d_p)$ is a function of particle diameter, α is the impact angle of the particle path with the wall face, $f(\alpha)$ is a function of impact angle, v is the relative velocity, $b(v)$ is a function of relative particle velocity, and A is the area of the cell face at the wall. The three functions C , f and b can be defined as boundary conditions at the wall; however the default values are not updated to reflect the material being used. Therefore, these parameters have to be updated for different materials. It is known that one of the main parameters which influence the erosion rate is the particles impingement angle. The impingement angle function can be used as the following model (Finnie, 1960; Mazur et al., 2004) and defined by a piece-linear profile

$$f(\alpha) = \sin(2\alpha) - 3\sin^2(\alpha) \quad \text{for } \alpha \leq 18.43^\circ \quad (28a)$$

$$f(\alpha) = \cos^2(\alpha)/3 \quad \text{for } \alpha > 18.43^\circ \quad (28b)$$

The accretion rate is given by

$$R_{\text{accretion}} = \sum_{p=1}^N \frac{\dot{m}_p}{A} \quad (29)$$

To calculate the erosion rate from Eq. (27), the diameter function and velocity exponent function are adopted as $1.8\text{E-}09$ and 1.73 (Fluent, 2006; Edwards et al., 2000; Edwards et al., 2001). The CFD model records the number, velocity, mass and the impact angle of the various particles for each of the grids that form the internal geometry of the hydrocyclone. Then, the erosion rate of the hydrocyclone walls is determined using Eqs. (27) and (28). There are many parameters affecting the erosion rate, such as flow rate, design of the inlet, geometry and dimensions of the hydrocyclone and slurry properties etc. can affect the erosion rate, among which the inlet has a very important effect on the wear characteristics of hydrocyclone. Thus, as a preliminary work, we will calculate erosion rate for hydrocyclone with four different inlets and discuss the influence of the design of inlet ducting on wear characteristics of hydrocyclone.

3. Simulation

The simulations are performed using Fluent CFD software package (version 6.3.26). As noted earlier published experimental data on a 75mm standard hydrocyclone is used to validate the CFD model. Figure 1 shows the dimensions and computational mesh for the test hydrocyclone ; Table 1 lists its geometrical parameters. The geometry used in the simulation is the same as that of the experiment (Hsieh, 1988); also the same area of quadrate inlet is used. Four turbulence models RNG k- ϵ , QPS RSM, and SLM and RNG LES were tested. In the simulation, the velocity inlet boundary condition and pressure outlet boundary conditions are applied for the vortex finder and the spigot. The inlet flow rate is 1.12 kg/s and the pressure at the two outlets is 1atm . The physical

constants for the liquid phase were set as those of water. The solid particle density is 2700 kg/m^3 and its mass fraction is 4.8% at the inlet. The unsteady solver with time steps $10^{-4} \sim 10^{-6} \text{ s}$ was applied in the simulations. The flow field reaches steady state after about 2s, therefore, the simulated results presented here are those for 3s after simulation starts i.e. when the flow is steady. The flow problem is simulated with three-dimensional unstructured mesh of hexahedral cells. Trial numerical results indicated that the solution is independent of the characteristics of the mesh size. Combined with the VOF model, the air core can be predicted with each one of the four turbulence models for comparison. The erosion rate of the hydrocyclone with four different inlets was also predicted with the RNG LES model.

Table 1.
Geometry of the 75mm standard hydrocyclone modeled

Parameter	Dimension
Diameter of hydrocyclone	75mm
Diameter of the inlet	25mm
Diameter of the vortex finder	25mm
Diameter of the spigot	12.5mm
Length of the cylindrical section	75mm
Length of the conical section	186mm
Length of vortex finder	50mm
Cone angle	20°

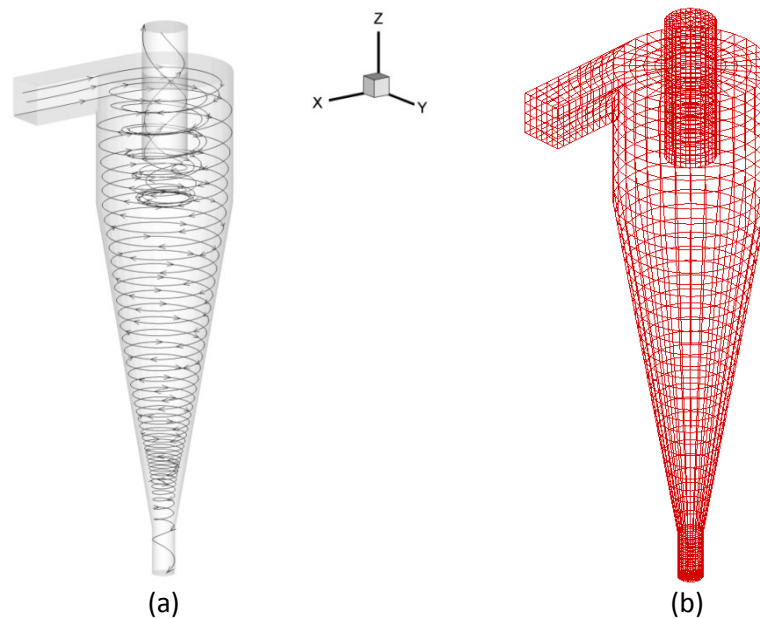


Fig. 1. (a) Schematic dimensions of the standard hydrocyclone with stream lines, (b) Grid representation used in simulation.

4. Model Validation

In this section, the simulated flow field, air core and particle classification results are compared with experiment (Hsieh, 1988) to validate the model. Moreover, a comparison between the experimental and the numerical results is also made for other variables of the hydrocyclone e.g. pressure drop and volume split ratio.

4.1 Fluid flow field

Fig. 1(a) shows several representative streamlines in a 75mm standard hydrocyclone. It clearly indicates swirling flow pattern, and splitting overflow and underflow in hydrocyclone. In order to explore the inner flow field in hydrocyclone, three different horizontal planes situated 60, 120 and 170mm from the top wall of 75mm standard hydrocyclone are selected to give a general description of velocity field. On each plane, the axial and tangential velocity profiles are compared with those of the experimental results.

Figs. 2 (a) and 2 (b) show the axial and tangential velocity profiles at 60mm from the top wall of the hydrocyclone, where four numerical results using RNG $k-\varepsilon$, QPS RSM, SLM LES and RNG LES turbulence models are compared with the experimental results. The four results are all close to the experimental ones, but the QPS RSM, SLM LES and RNG LES computations track the axial and tangential velocities more closely than the RNG $k-\varepsilon$ one. It can be seen clearly that the predicted axial and tangential velocities near the wall are near zero because the no-slip boundary condition is used for the walls. For the axial velocity near wall, there is little difference between the numerical results and the experimental ones, while for tangential velocity, the experimental value is nearly zero which is the same as numerical result. Also, because of the air core, the axial velocity near the central core of the hydrocyclone is quite high while the tangential velocity approaches 0, which are all consistent with the experimental results and the physical conditions.

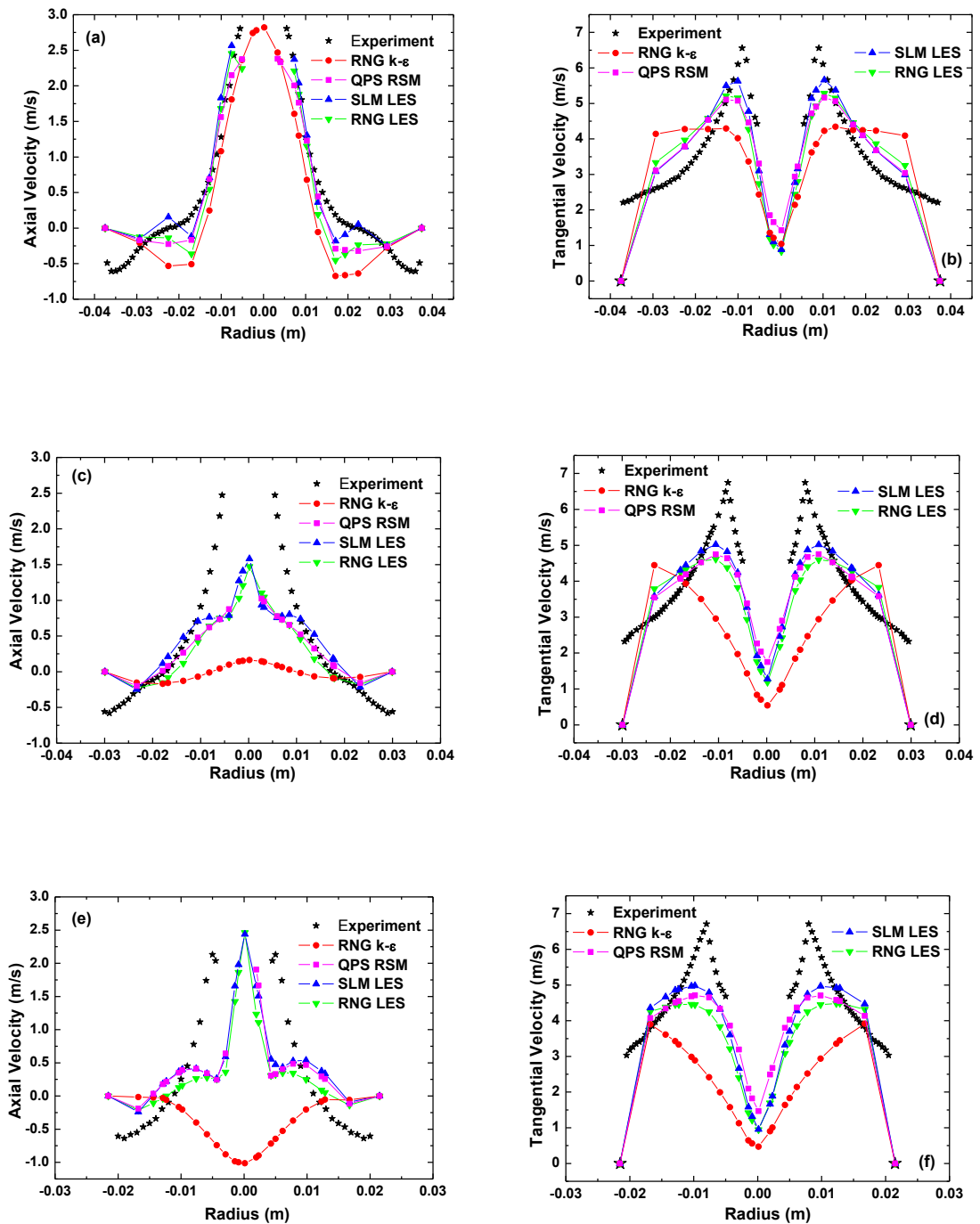


Fig. 2. Axial and tangential velocity profile- comparison with experimental results at (a)-(b) 60mm, (c)-(d) 120mm, and (e)-(f) 170mm from the top wall of 75mm standard hydrocyclone.

Figs. 2 (c) and (d) describe the axial and tangential velocity profiles in the 120 mm plane. The difference between the predicted velocities with RNG k-ε model and those of experiment is so large that it may be concluded that the RNG k-ε model is not suitable for modeling the turbulent

flow in a hydrocyclone. The predicted results of QPS RSM, SLM LES and RNG LES models are all similar to each other, and rather close to the experimental values. The predicted behavior near the wall and at the center of hydrocyclone is the same as that along the 60 mm plane.

Figs. 2 (e) and (f) display the axial and tangential velocity profiles in the 170mm plane. The predicted axial velocity with RNG $k-\epsilon$ model is contrary to the experimental results (see Fig. 2 (e)). This can be explained from the fact that the flow near the central zone of the hydrocyclone is drained off due to the underflow because of the disappearance of the air core (see Fig. 3), hence the predicted axial velocity approaches negative values. The close performances of QPS RSM, SML LES and RNG LES models can be found in Figs. 2 (e) and (f), which can better predict the turbulent flow in the hydrocyclone.

From above comparisons, it is seen that the predicted axial and tangential velocities of the RNG $k-\epsilon$ turbulence model are far from the experimental results while the performances of QPS RSM, SML LES and RNG LES models are close to each other and the experimental results. Therefore, we conclude that the RNG $k-\epsilon$ model is not suitable for modeling hydrocyclones while QPS RSM, SML LES and RNG LES models can capture the velocity profiles at different locations of the flow and can be used to model the hydrocyclone. Comparison between the latter three turbulence models indicates that although the QPS RSM and SML LES models perform better near the center, the RNG LES model can track the turbulent velocities near the wall better. Furthermore, the approximated no slip boundary condition is also suitable for hydrocyclone modeling. Another point should be noted that the QRS RSM turbulence model combining with VOF multiphase model can lead to numerical stability, while the LES model consumes significantly more computing resources and times.

4.2 Formation of the air core

The ability to predict well the development of the air core in the hydrocyclone is a test of the CFD model. Figs. 3-6 show the predicted air core formation with RNG $k-\epsilon$, QPS RSM, SLM LES and RNG LES turbulence models, respectively. Figure 3 indicates the evolution of the air volume fraction with the RNG $k-\epsilon$ model at real times from 0.02s to 3.0s. The variable of air volume fraction in the first second is distinct and then the air fraction changes are very minor. After the first second, a little change in the air volume fraction can be only found at the top end of hydrocyclone in the following one second. Between 2s to 3s, there is no variability of the air volume fraction. Further simulations indicate that the flow varies little after 1s and reaches steady state after 2s. It can be seen from Fig. 3 that the air core is formed at about 0.6s and then disappears; the predicted air core diameter with RNG $k-\epsilon$ model is 0.2. The numerically computed air core diameter of Delgadillo et al. (2005, 2006) with RNG $k-\epsilon$ model is 0, which is much closer to the current results. Thus, the RNG $k-\epsilon$ model can not predict the air core in a hydrocyclone, which is its major weakness.

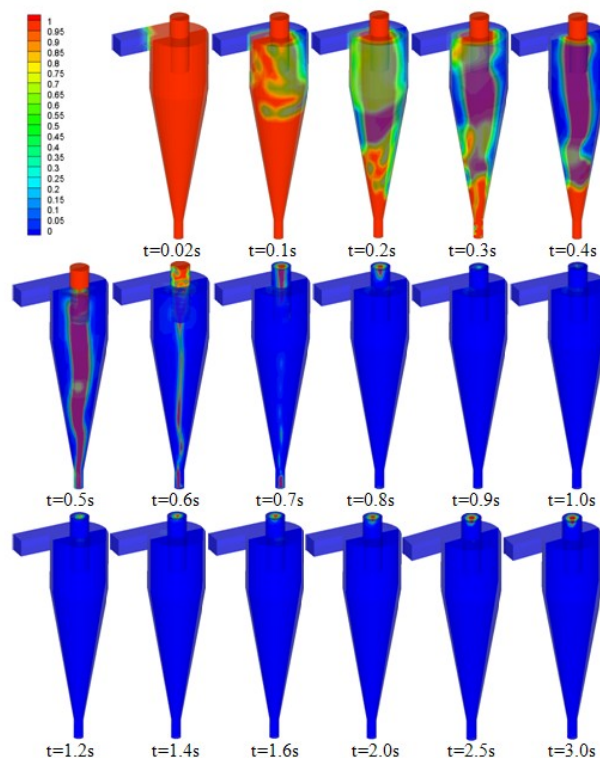


Fig. 3. The predicted air volume fraction and air core formation with RNG $k-\epsilon$ turbulence model from time 0-3s.

Fig. 4 exhibits the air core formation with the QPS RSM turbulence model. The air core is formed in the first second and remains steady after 2s. A nearly parabolic shape of the air core is well predicted by QPS RSM turbulence model, which agrees well with the experimental data. The predicted air core diameter is about 10.6 mm, which is very close to the experimental value of 10mm. Figs. 5 and 6 show the air core development with SLM and RNG LES turbulence models. The similar formation process as QPS RSM model can be found in Figs. 5 and 6. Comparing with the air core with RSM model, the shape of air with LES is more regular and closer to the experimental shape. The predicted diameter is 11.5 and 10.45mm for SLM LES and RNG LES respectively. The error of SLM LES is large than 10%, and that of RNG LES is less than 5%.

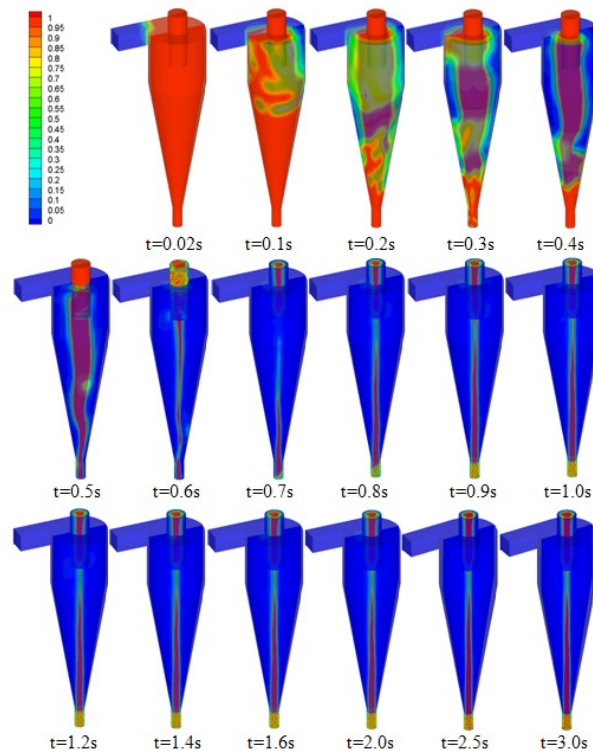


Fig. 4. The predicted air volume fraction and air core formation with QPS RSM turbulence model from time 0-3s.

The general mass balances are also calculated and compared with experiments as listed in Table 2. The experimental split ratio of the 75mm standard hydrocyclone is 95.1%, while the predicted split ratio with the RNG k- ϵ , QPS RSM, SLM LES and RNG LES turbulence models is 78.75%, 95.7%,

M3TC Technical Report TN-08-01

95.6% and 92%, respectively. For pressure drop, the experimental result is 46.7kPa, while the numerical results are 38.3, 41.1, 40.2 and 38.4 kPa, respectively. The experimental and numerical air core diameters are also listed in Table 2. In all, QPS RSM, SLM LES and RNG LES can be used for modeling a hydrocyclone. Considering numerical stability of RSM and relatively high accuracy near the wall of RNG LES turbulence model, the RNG LES will be adopted in the calculating erosion rate of hydrocyclone.

Table 2.
General mass balance for four different turbulent models

	Experiment	RNG k- ϵ	QPS RSM	SLM LES	RNG LES
Feed flow rate (kg/s)	1.117	1.12	1.12	1.12	1.12
Overflow flow rate (kg/s)	1.062	0.882	1.072	1.071	1.03
Underflow flow rate (kg/s)	0.055	0.238	0.058	0.053	0.09
Split ratio (%)	95.1	78.75	95.7	95.6	92.0
Pressure drop (kPa)	46.7	38.3	41.13	40.2	38.4
Air core diameter (mm)	10.0	0.2	10.6	11.5	10.45

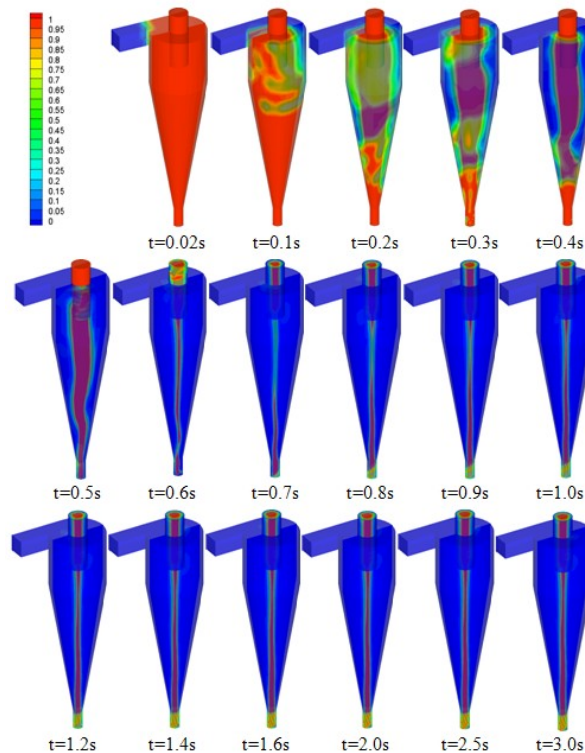


Fig. 5. The predicted air volume fraction and air core formation with SLM LES turbulence model from time 0-3s.

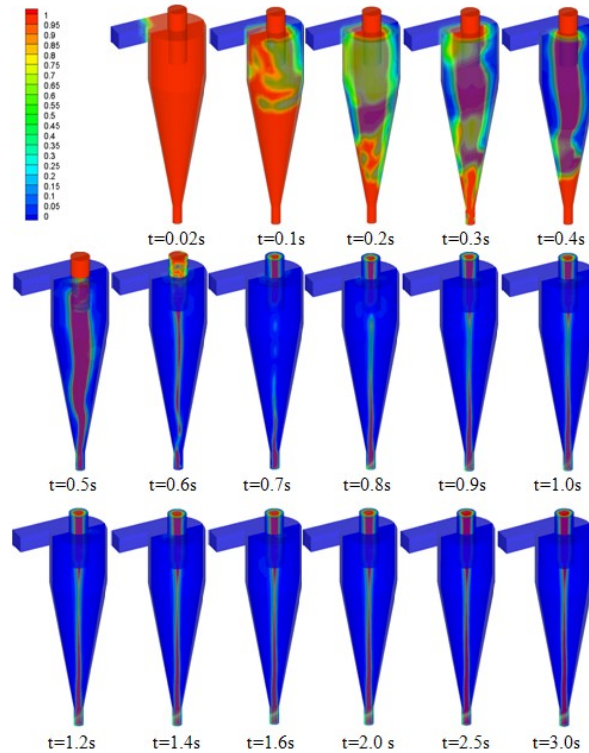


Fig. 6. The predicted air volume fraction and air core formation with RNG LES turbulence model from time 0-3s.

5. Erosion Rate

There are many parameters and conditions affecting the erosion rate of the hydrocyclone; one of the important ones is the geometry of the feed inlet. Although the standard inlet as shown in Fig. 7(a) is very common in mineral processing, it does not perform so well in wear resistance despite its popularity. Therefore, three hydrocyclones with different inlets were tested for the erosion rate they are subject to with all parameters being fixed. Fig. 7 shows the detailed inlet geometry and dimension for the four cases. In order to compare the effect of the inlet geometry on the erosion rate, the same fluid and particle velocity 2.25m/s are adopted for each case, the flow rate of solid particles is set as 0.05kg/s, particle diameter is 11.5 μ m. In calculation of the erosion rate of hydrocyclone, the interactions of the solid particles and the continuous phase need to be taken into account.

Fig.8 displays the variations of erosion rate of standard hydrocyclone (Fig. 7(a)) with time from 0.1s to 0.9s. At the beginning, the erosion rate on the wall of hydrocyclone is not very obvious because the solid particles have not yet reached the inner body of the device (fig. 8(a)). With the particles injected into the device, more and more particles collide the wall inducing distinct wear (fig. 8(b)). Two wear “hot spots” can be found at the intersection of the cylindrical and conical sections and the middle part of conical section. At the hot spot in the middle part of conical section, the erosion rate is more than $1E-4 \text{ kg}/(\text{m}^2\text{s})$, which is a very high value. Thus, this hot spot will cause device failure. After 0.1 second, wear occurs at vortex finder and spigot as well, and the latter is more obvious than the former one. Note that the erosion rates at the bottom of conical and spigot are very high. From 0.2s, the bottom of vortex finder begins to appear wear zone, and from 0.3s the wear phenomena of vortex finder is more and more distinct with increasing finer ores escape from it. It can be seen from fig. 8 that there is hardly any wear in the inlet ducting. The erosion rate variation in the first 0.2s is very sharp but the development later on is not obvious.

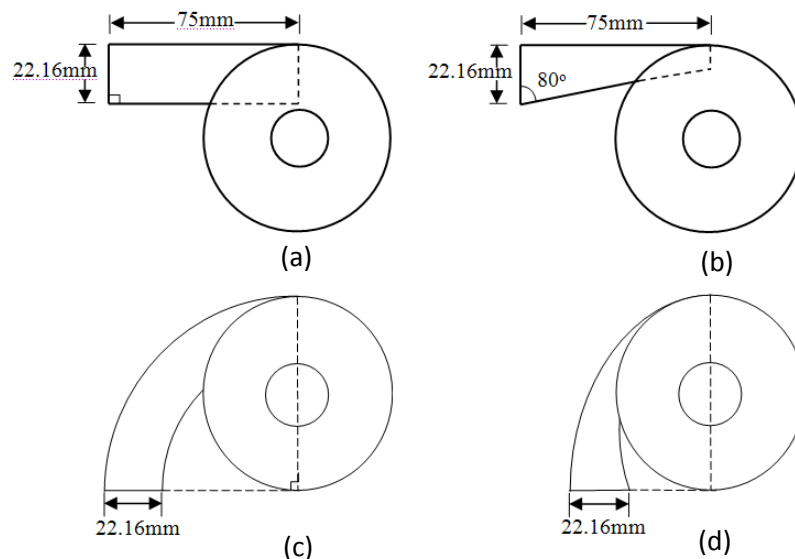


Fig.7. Four hydrocyclones with different inlet duct designs: (a) standard tangential inlet, (b) modified tangential inlet, (c) circular involute inlet and (d) elliptical involute inlet.

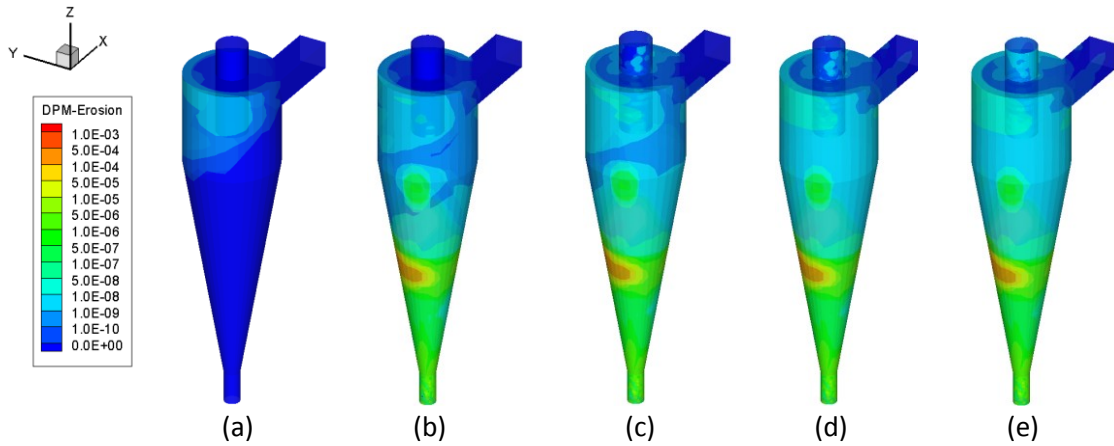


Fig. 8. Surface plots of the computed local erosion rates in the modeled hydrocyclone with a standard tangential inlet at various times: (a) 0.1s, (b) 0.2s, (c) 0.3s, (d) 0.6s and (e) 0.9s.

Fig. 9 shows the erosion rate of the inner wall of the simulated hydrocyclones fitted with different inlets. Table 3 lists the maximum and average erosion rates and computed pressure drop for each case. Although the standard hydrocyclone with tangential inlet (fig. 9(a)) has been widely used in mineral processes, the erosion rate for it is the highest compared with the other three designs. Also, obvious wear hot spot can be found at the bottom of the cone section, where the erosion rate is very high. The maximum and integral erosion rates are $3.72\text{E-}4$ and $1.87\text{E-}6$ $\text{kg}/(\text{m}^2\text{s})$, respectively. However, the pressure drop is the lowest, 32.8 kPa. For the modified tangential inlet (fig. 9(b)), there is no obvious wear hot spot, but the erosion rate is still high compared with the involute inlet. The maximum and average erosion rates are $7.61\text{E-}7$ and $4.72\text{E-}8$ $\text{kg}/(\text{m}^2\text{s})$, respectively, and the pressure drop is very high (81.7kPa). For the involute inlet which can provide a smooth transition from pressure energy to rotational momentum, the distribution of erosion rate is relatively uniform and the value is low. For the circular involute inlet, the maximum computed erosion rate is only $4.32\text{E-}7$ $\text{kg}/(\text{m}^2\text{s})$ and the average value is $2.91\text{E-}8$ $\text{kg}/(\text{m}^2\text{s})$ while for the elliptical involute inlet, the maximum and integral erosion rates are $4.37\text{E-}7$ and $3.90\text{E-}8$ $\text{kg}/(\text{m}^2\text{s})$, respectively. Moreover, the pressure drop of circular involute inlet (45.7kPa) is much smaller than that of elliptical involute inlet (72.3kPa). It can be seen from fig. 9 that the erosion rate at the inlet is nearly zero, while the erosion rate for conical section and spigot is much higher than that of cylindrical section and vortex finder.

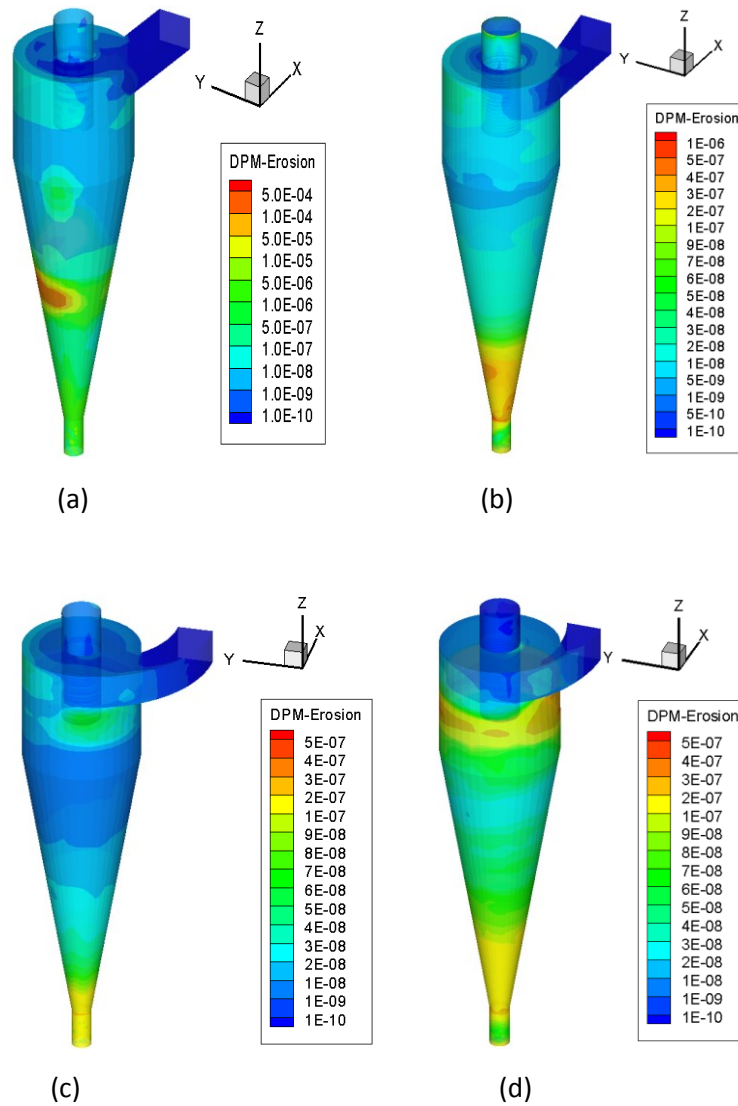


Fig.9. Computed local erosion rates of the inner wall of tested hydrocyclone fitted with different inlets: (a) standard tangential inlet, (b) modified tangential inlet, (c) circular involute inlet and (d) elliptical involute inlet.

Table 3.
Computed Erosion rate for four inlet duct designs

Inlet	Pressure drop (kPa)	Maximum Erosion rate (kg/(m ² s))	Face average erosion rate (kg/(m ² s))
Standard tangential inlet	32.8	3.72E-4	1.84E-6
Modified tangential inlet	81.7	7.62E-7	4.72E-8
Circular involute inlet	45.7	4.32E-7	2.91E-8
Elliptical involute inlet	72.3	4.37E-7	3.90E-8

6. Concluding Remarks

M3TC Technical Report TN-08-01

Four turbulence models, RNG k- ϵ , QPS RSM, SLM LES and RNG LES, were used to predict the aerodynamic performance of a 75mm standard hydrocyclone. The comparison of numerical and experimental results indicates that the RNG k- ϵ turbulence model is not suitable for modeling highly swirling flows in hydrocyclones, while QPS RSM, SML LES and RNG LES models can capture well the velocity profiles and predict the formation of air core. With a VOF multiphase model, the air core formation was analyzed in detail and the diameter of steady air core was successfully predicted. The effects of inlet on the erosion rate were investigated with the RNG LES model. The involute inlet can eliminate the wear hot spot and lower the level of concentrated wear. This is only a preliminary study of the design and optimization process concerning erosion rate of a hydrocyclone. In our future study, other parameters and conditions such as inlet flow rate, particle characteristics etc. which can affect erosion rate will be investigated as all of the performance parameters should be taken into account for good design and operation of the hydrocyclone and to increase its service life.

Acknowledgments

This work was supported by the Economic Development Board at M3TC of NUS.

References

- Amezcuca, A.C., Muñoz, A.G., Romero, C.A., Czerwicz, Z.M., Amezcuca, R.C., 2007. Numerical investigation of the solid particle erosion rate in a steam turbine nozzle. *Applied Thermal Engineering* 27, 2394-2403.
- Boysan, F., Ayers, W.H., Swithenbank, J., 1982. Fundamental mathematical-modelling approach to cyclone design. *Chemical Engineering Research and Design* 60, 222-230.
- Bozzini, B., Ricotti, M.E., Boniardi, M., Mele, C., 2003. Evaluation of erosion-corrosion in multiphase flow via CFD and experimental analysis. *Wear* 255, 237-245.
- Bradley, D., 1965. *The Hydrocyclone*, Pergamon Press, London.

M3TC Technical Report TN-08-01

- Brennan, M., 2006. CFD simulations of hydrocyclones with an air core: Comparison between large eddy simulations and a second moment closure. *Chemical Engineering Research and Design* 84, 495-505.
- Chen, X., McLaury, B.S., Shirazi, S.A., 2004. Application and experimental validation of a computational fluid dynamics (CFD)-based erosion prediction model in elbows and plugged tees. *Computers & Fluids* 33, 1251-1272.
- Cullivan, J.C., Williams, R.A., Cross, C.R., 2003. Understanding the hydrocyclone separator through computational fluid dynamics. *Chemical Engineering Research and Design* 81, 455-465.
- Cullivan, J.C., Williams, R.A., Dyakowski, T., Cross, C.R., 2004. New understanding of a hydrocyclone flow field and separation mechanism from computational fluid dynamics. *Minerals Engineering* 17, 651-660.
- Dabir, B., Petty, C.A., 1986. Measurement of mean velocity profiles in a hydrocyclone using laser Doppler anemometry. *Chemical Engineering Communications* 48, 377-388.
- Dai, G.Q., Chen, W.M., Li, J.M., Chu, L.Y., 1999. Experimental study of solid-liquid two-phase flow in a hydrocyclone. *Chemical Engineering Journal* 74, 211-216.
- Delgadillo, J.A., Rajamani, R.K., 2005. A comparative study of three turbulence-closure models for the hydrocyclone problem. *International Journal of Mineral Processing* 77, 217-230.
- Delgadillo, J.A., 2006. Modeling of 75- and 250mm Hydrocyclones and Exploration of Novel Designs Using Computational Fluid Dynamics. PhD Thesis, University of Utah, USA.
- Delgadillo, J.A., Rajamani, R.K., 2007. Exploration of hydrocyclone designs using computational fluid dynamics. *International Journal of Mineral Processing* 84, 252-261.
- Edwards, J.K., McLaury, B.S., Shirazi, S.A., 2000. Evaluation of alternative pipe bend fittings in erosive service. *Proceedings of ASME FEDSM'00: ASME 2000 Fluids Engineering Division Summer Meeting, Boston, FEDSM 2000-11251*.
- Edwards, J.K., McLaury, B.S., Shirazi, S.A., 2001. Modeling solid particle erosion in elbows and plugged tees. *Journal of Energy Resources Technology* 123, 277-284.
- Finnie, I., 1960. Erosion of surfaces by solid particles. *Wear* 3, 87-103.
- Fluent V6.3, 2006. User's guide. Fluent Inc., Centerra Resource Park, 10 Cavendish Court, Lebanon NH 03766.
- Fraser, S.M., Rasek, A.M., Abdel, Abdullah, M.Z., 1997. Computational and experimental investigations in a cyclone dust separator. *Journal of Process Mechanical Engineering* 211, 247-257.
- He, P., Salcudean, M., Gartshore, I.S., 1999. A numerical simulation of hydrocyclones. *Chemical Engineering Research and Design* 77, 429-441.

M3TC Technical Report TN-08-01

- Hsieh, K.T., 1988. Phenomenological Model of the Hydrocyclone. Ph.D. Thesis, The University of Utah, Salt Lake City, UT, USA.
- Hsieh, K.T., Rajamani, R.K., 1991. Mathematical-model of the hydrocyclone based on physics of fluid-flow. *AIChE Journal* 37, 735-746.
- Huang, L.X., Kumar, K., Mujumdar, A.S., 2003. A parametric study of the gas flow patterns and drying performance of co-current spray dryer: Results of a computational fluid dynamics study. *Drying Technology* 21, 957-978.
- Huang, L.X., Kumar, K., Mujumdar, A.S., 2004. Simulation of a spray dryer fitted with a rotary disk atomizer using a three-dimensional computational fluid dynamic model. *Drying Technology* 22, 1489-1515.
- Huang, L.X., Mujumdar, A.S., 2006. Numerical study of two-stage horizontal spray dryers using computational fluid dynamics. *Drying Technology* 24, 727-733.
- Launder, B.E., Reece, G.J., Rodi, W., 1975. Progress in the development of a Reynolds—stress turbulence closure. *Journal of Fluid Mechanics* 68, 537-566.
- Lilge, E.O., 1962. Hydrocyclone fundamentals. *Transactions Institution Mining Metallurgy* 71, 285-337.
- Ma, L., Ingham, D.B., Wen, X., 2000. Numerical modelling of the fluid and particle penetration through small sampling cyclones. *Journal of Aerosol Science* 31, 1097-1119.
- Mazur, Z., Campos-Amezcuca, R., Urquiza-Beltrán, G., García-Gutiérrez, A., 2004. Numerical 3D simulation of the erosion due to solid particle impact in the main stop valve of a stream turbine. *Applied Thermal Engineering* 24, 1877-1891.
- Monredon, T.C., Hsieh, K.T., Rajamani, R.K., 1992. Fluid-flow model of the hydrocyclone—an investigation of device dimensions. *International Journal of Mineral Processing* 35, 65-83.
- Narasimha, M., Sripriya, R., and Banerjee, P.K., 2005. CFD modelling of hydrocyclone—prediction of cut-size. *International Journal of Mineral Processing* 71, 53–68.
- Narasimha, M., Brennan, M., Holtham, P.N., 2006. Large eddy simulation of hydrocyclone—prediction of air-core diameter and shape. *International Journal of Mineral Processing* 80, 1-14.
- Nowakowski, A.F., Cullivan, J.C., Williams, R.A., Dyakowski, T., 2004. Application of CFD to modeling of the flow in hydrocyclones. Is this a realizable option or still a research challenge? *Minerals Engineering* 17, 661-669.
- Olson, T.J., Van Ommen, R., 2004. Optimizing hydrocyclone design using advanced CFD model. *Minerals Engineering* 17, 713-720.
- Rajamani, R.K., Devulapalli, B., 1994. Hydrodynamics modeling of swirling flow and particle classification in large-scale hydrocyclones. *KONA Powder and Particle Journal* 12, 95-103.

- Schuetz, S., Mayer, G., Bierdel, M., Piesche, M., 2004. Investigations on the flow and separation behaviour of hydrocyclones using computational fluid dynamics. *International Journal of Mineral Processing* 73, 229–237.
- Sciubba, E., Zeoli, N., 2007. A study of sootblower erosion in waste-incinerating heat boilers. *Journal of Energy Resources Technology* 129, 50-53.
- Slack, M.D., Del Porte, S., Engelman, M.S., 2003. Designing automated computational fluid dynamics modeling tools for hydrocyclone design. *Minerals Engineering* 17, 705-711.
- Smagorinsky, J., 1963. General circulation experiments with the primitive equations: I. The basic experiment. *Monthly Weather Review* 91, 99-164.
- Souza, F.J., Neto, A.S., 2004. Preliminary results of large eddy simulation of a hydrocyclone. *Thermal Engineering* 3, 168-173.
- Speziale, C.G., Sarkar, S., Gatski, T.B., 1991. Modelling the pressure strain correlation of turbulence: an invariant dynamical systems approach. *Journal of Fluid Mechanics* 227 (1991) 245-274.
- Suasnabar, D.J., 2000. Dense Medium Cyclone Performance, enhancements via computational modeling of the physical process. PhD Thesis, University of New South Wales.
- Svarovsky, L., 1984. *Hydrocyclones*. Holt, Rinehart and Winston.
- Wang, B., Chu, K.W., Yu, A.B., 2007. Numerical study of particle—Fluid flow in hydrocyclone. *Industrial & engineering chemistry research* 46, 4695-4705.
- Yakhot, A., Ozag, S.A., 1986. Renormalization group analysis of turbulence: I. Basic theory. *Journal of Scientific Computing* 1, 1–51.
- Yakhot, A., Ozag, A., Yakhot, V., Israeli, M., 1989. Renormalization group formulation of large eddy simulations. *Journal of Scientific Computing* 4, 139-158.
- Yoshioka, N., Hotta, Y., 1955. Liquid cyclone as a hydraulic classifier. *Chemical Engineer of Japan*. 19, 633-641.